

Nonlinear Cherenkov difference-frequency generation exploiting birefringence of KTP

R. Ni, L. Du, Y. Wu, X. P. Hu, J. Zou, Y. Sheng, A. Arie, Y. Zhang, and S. N. Zhu

Citation: [Applied Physics Letters](#) **108**, 031104 (2016); doi: 10.1063/1.4940095

View online: <http://dx.doi.org/10.1063/1.4940095>

View Table of Contents: <http://scitation.aip.org/content/aip/journal/apl/108/3?ver=pdfcov>

Published by the [AIP Publishing](#)

Articles you may be interested in

[Optical parametric generation in periodically poled K Ti O P O 4 via extended phase matching](#)

Appl. Phys. Lett. **91**, 131120 (2007); 10.1063/1.2790825

[Ultrabroad-band phase matching in two recently grown nonlinear optical crystals for the generation of tunable ultrafast laser radiation by type-I noncollinear optical parametric amplification](#)

J. Appl. Phys. **94**, 1329 (2003); 10.1063/1.1591074

[Erratum: "Tunable midinfrared source by difference frequency generation in bulk periodically poled KTiOPO 4" \[Appl. Phys. Lett. 74, 914 \(1999\)\]](#)

Appl. Phys. Lett. **74**, 2723 (1999); 10.1063/1.123950

[Tunable midinfrared source by difference frequency generation in bulk periodically poled KTiOPO 4](#)

Appl. Phys. Lett. **74**, 914 (1999); 10.1063/1.123408

[Phase-matched mid-infrared difference frequency generation in GaAs-based waveguides](#)

Appl. Phys. Lett. **71**, 3622 (1997); 10.1063/1.120460

The advertisement features a photograph of the Lake Shore Model 372 cryogenic temperature controller, a white rectangular device with a digital display and control buttons. The display shows '96.837'. To the right, a detailed cutaway view of a cryogenic system is shown, revealing internal components like a cryostat and various tubes. The Lake Shore CRYOTRONICS logo is in the top right corner.

Precise temperature control
for **cryogenic research**

Model 372

Lake Shore
CRYOTRONICS

Nonlinear Cherenkov difference-frequency generation exploiting birefringence of KTP

R. Ni,¹ L. Du,¹ Y. Wu,¹ X. P. Hu,^{1,a)} J. Zou,¹ Y. Sheng,² A. Arie,³ Y. Zhang,¹ and S. N. Zhu¹

¹National Laboratory of Solid State Microstructures and School of Physics, Nanjing University, Nanjing 210093, China

²Laser Physics Center, Research School of Physics and Engineering, Australian National University, Canberra ACT 0200, Australia

³School of Electrical Engineering, Faculty of Engineering, Tel-Aviv University, Tel-Aviv 69978, Israel

(Received 2 November 2015; accepted 5 January 2016; published online 19 January 2016)

In this letter, we demonstrate the realization of nonlinear Cherenkov difference-frequency generation (CDFG) exploiting the birefringence property of KTiOPO₄ (KTP) crystal. The pump and signal waves were set to be along different polarizations, thus the phase-matching requirement of CDFG, which is, the refractive index of the pump wave should be smaller than that of the signal wave, was fulfilled. The radiation angles and the intensity dependence of the CDFG on the pump wave were measured, which agreed well with the theoretical ones. © 2016 AIP Publishing LLC.

[<http://dx.doi.org/10.1063/1.4940095>]

In particle physics, a charged particle moving faster than the speed of light will drive the medium to emit coherent light, and this is called Cherenkov radiation.¹ This concept can be extended to nonlinear optics as the nonlinear Cherenkov radiation, which is, when the phase velocity of the nonlinear polarization wave (v_p) driven by the incident light is faster than that of the harmonic wave (v), the harmonic wave will emit along the Cherenkov angle $\theta = \arccos(v/v_p)$. In 1970, Tien *et al.* observed the first Nonlinear Cherenkov radiation in a planar waveguide.² Since then, extensive works have been reported, including Cherenkov sum-frequency generation (SFG), third harmonic generation (THG), and high-order HG (HHG),^{3–10} which provide a promising route to produce short-wavelength lasers and broad-band frequency converters. Besides, Cherenkov second-HG (CSHG)¹¹ has some applications such as optical imaging of ferroelectric domain walls.^{12,13} In contrary to Cherenkov frequency up-conversion, Cherenkov down-conversion cannot be automatically realized because the phase velocity of the nonlinear polarization wave is generally smaller than that of the harmonic wave if the interacting waves are of the same polarization. Chen *et al.*¹⁴ demonstrated the realization of Cherenkov difference-FG (CDFG) in a two-dimensional periodically poled LiTaO₃ (PPLT), where the backward reciprocal vector was used to accelerate the nonlinear polarization wave. Birefringence properties in LiNbO₃ were previously used for demonstrating frequency up-conversion Cherenkov process.¹⁵ Here, we use a similar concept in KTiOPO₄ (KTP) but this time to generate a Cherenkov down-conversion process.

The difference-frequency generation considered in this work is a degenerate process (where the wavelength of signal equals that of idler) and the wave-vector mismatch of this process is $\Delta k = k_p - k_s - k_i = k_p - 2k_s = 4\pi(n_p - n_s)/\lambda_s$ (where the footnotes p , s , and i denote the pump, signal, and idler waves, respectively). To get a radiated signal wave, the

wave-vector mismatch should be less than zero, which requires that $n_p < n_s$. However, in normally dispersive media, n_p is always larger than n_s when they have the same polarizations. If the pump and the signal waves are chosen to be of different polarizations, the requirement may be met.

For the birefringent crystal KTP, Figure 1(a) shows the dispersion relations of the pump wave polarizing along the x direction and the signal/idler wave polarizing along the z direction at room temperature, respectively.¹⁶ From the figure, we can see that, when the pump wavelength is longer than about 370 nm, the refractive index of pump is always lower than that of the signal or idler wave. Thus, the wave vector mismatch for the DFG process is less than zero, i.e., $\Delta k = k_p - 2k_s < 0$, just as shown in Figure 1(b).

The experimental setup is shown in Figure 2. The two ports of the laser can export 1064 nm wave (polarizing along the z -direction) and 532 nm wave (polarizing along the x -direction), respectively, with a repetition rate of 10 Hz and a pulse width of 20 ps. Polarization of both beams were rotated by 90° with a half-wave plate. A prism was put into the path to ensure an optimal temporal overlap of the two pulses. The incident beams were loosely focused inside the crystal with a beam waist of about 100 μm . The crystal used in the experiment is a 0.5-mm-long one-dimensional PPKTP with a poling period of about 15 μm and the group velocity mismatch between the short pulses is negligible within such a short interaction length. The domain walls of KTP parallel to the incident wave were not involved in the nonlinear frequency conversion process. Instead, the presence of the domain walls was to enhance the Cherenkov radiation.^{12,17}

First, we opened the port 1, letting the z -polarized 1064 nm wave incident into the PPKTP crystal along y axis. On the screen, a green spot labeled as ① and an ultraviolet (UV) spot labeled as ② (visualized with fluorescent powder) can be clearly observed, as shown in Figure 3(a). Spot ① is the direct CSHG process, polarizing along z -axis. The UV spot ② is a third harmonic generation of the incident IR beam via sum-frequency generation of the aforementioned

^{a)}Author to whom correspondence should be addressed. Electronic mail: xphu@nju.edu.cn.

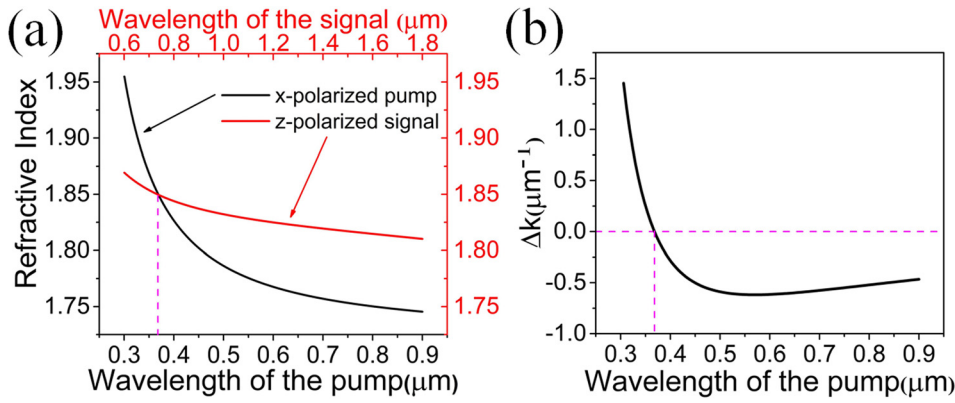


FIG. 1. (a) Theoretical refractive index of KTP. The black line represents the dispersion of x -polarized pump wave and the red represents that of the z -polarized signal wave. (b) The phase mismatch versus the wavelength of the pump. Curve under the horizontal zero line corresponds to the region, where the phase-matching condition of CDFG is met.

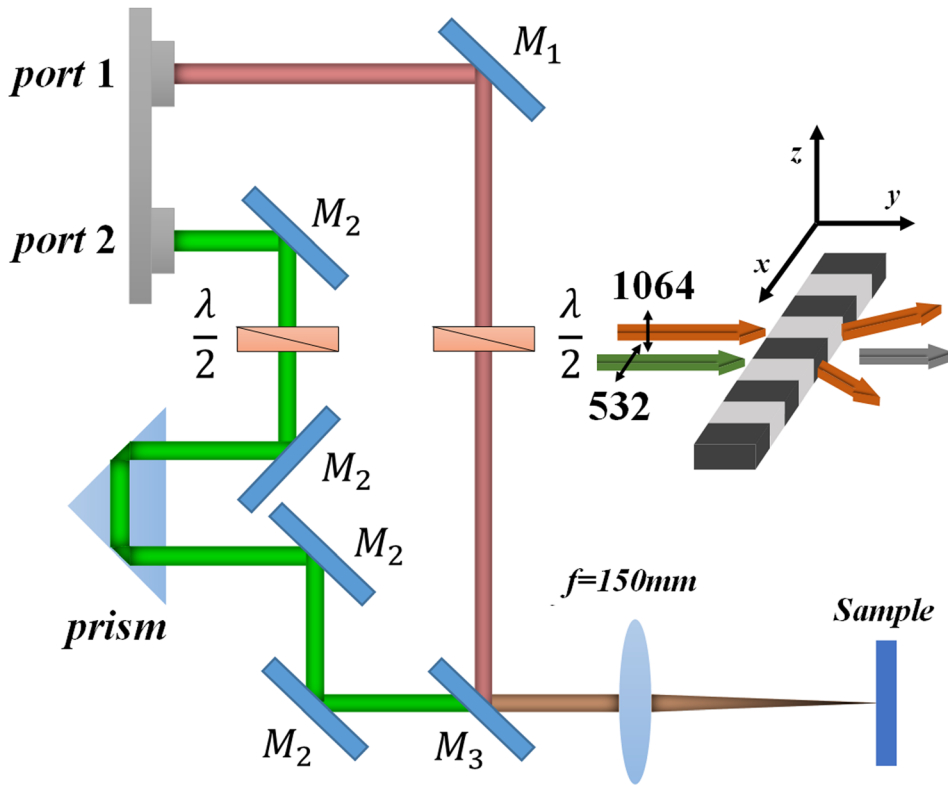


FIG. 2. Schematic experimental setup. M_1 : High-reflection at 1064 nm/45°, M_2 : High-reflection at 532 nm/45°, M_3 : High-reflection at 1064 nm and High-transmission at 532 nm. $\lambda/2$: half-wave plate for 1064 and 532 nm, respectively. f : lens with a focal length of 15 cm. The inset is sample setup.

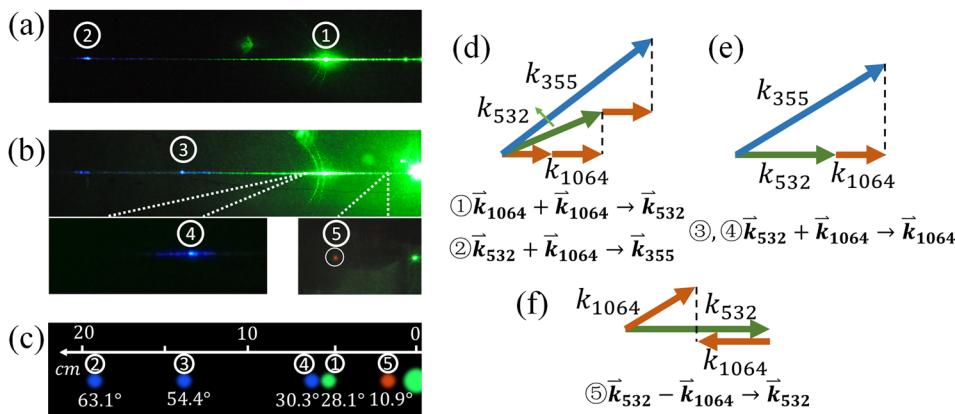


FIG. 3. The radiations projected on the screen when only z -polarized 1064 nm wave incident into the crystal (a), when the 532 nm and 1064 nm were mixed into the crystal (b); the schematic of all the five spots together with the corresponding measured Cherenkov radiation angles (c); the phase-matching diagrams of spots ① and ② (d), ③ and ④ (e), and ⑤ (f).

Cherenkov second-harmonic generation wave and the fundamental wave, and it is polarized along z -axis. The phase-matching diagram of spot ② is shown in Figure 3(d).

Subsequently, we opened the two ports and adjusted the prism to ensure the maximum overlap between the pump and the signal. Besides spots ① and ②, one more CTHG spot

(labeled as ③) appeared on the screen (shown in Figure 3(b)), which was polarized along z -direction and generated by Cherenkov sum-frequency mixing of the collinear z -polarized signal and the z -polarized pump waves. When a filter was used to reflect the shining 532 nm green light, another UV spot (labeled as ④) can be observed. Spot ④ was

TABLE I. The non-zero electrical field (E) components of the interacting waves for generating the five spots and the corresponding second-order nonlinear coefficient involved.

Spot number	Non-zero components of E		Nonlinear coefficient
①	$E_z(1064)$	$E_z(1064)$	d_{33}
②	$E_z(1064)$	$E_z(532)$	d_{33}
③	$E_z(1064)$	$E_z(532)$	d_{33}
④	$E_z(1064)$	$E_x(532)$	d_{15}
⑤	$E_z(1064)$	$E_x(532)$	d_{15}

x -polarized and was generated by a Cherenkov sum-frequency process between the z -polarized signal at 1064 nm and x -polarized pump at 532 nm, and Figure 3(e) shows the phase-matching diagram of this type of Cherenkov THG (spots ③ and ④). With the help of an IR viewing card, at a relatively small angle, one x -polarized infrared Cherenkov spot (labeled as ⑤) was observed, generated by the Cherenkov difference-frequency interaction between the z -polarized signal and the x -polarized pump waves. This spot was measured to be x -polarized and the wavelength was 1064 nm. Combining with the measured radiation angle, we found that this IR spot was generated through the DFG process between incident 1064 and 532 nm beams at different polarizations. The average output power of the CDFG was measured to be about 10 μ W and the corresponding powers of the pump and the signal waves were 0.7 and 3.8 mW, respectively. Therefore, a birefringence controlled CDFG was realized in the PPKTP, just as predicted in the foregoing analysis.

The abovementioned five spots were generated from interacting waves with different polarizations, thus different second-order optical nonlinear coefficients were responsible for these observed processes. Taking into consideration the second-order nonlinear optical susceptibility tensor of KTP¹⁸ and the non-zero components of the electrical fields of the interacting waves, the nonlinear coefficient responsible for each process is listed in Table I.

The external radiation angles of all the five spots are given in Table II. Using the refractive index of KTP in Ref. 16, the theoretical predictions of the radiation angles are also listed in the table and match well with the experimental values.

In theory, the intensity of CDFG is proportional to the product of the intensity of the pump I_{pump} and the intensity of the signal I_{signal}

$$I_{idler} \propto d_{15}^2 I_{pump} I_{signal} L^2 \times \sin^2(\Delta k_L L),$$

where Δk_L is the longitudinal phase-mismatch parallel to the propagation direction of the incident waves. L is the

TABLE II. Experimental and theoretical results of the external radiation angles.

	Spot ①	Spot ②	Spot ③	Spot ④	Spot ⑤
Experimental	28.1°	63.1°	54.4°	30.3°	10.9°
Theoretical	27.5°	62.3°	52.5°	29.4°	11.5°

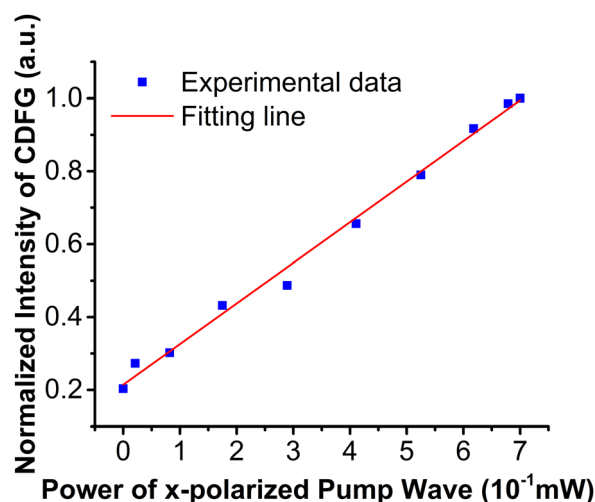


FIG. 4. The power dependence of the CDFG on the x -polarized pump wave.

interaction length, and theoretically, the output of the idler wave is proportional to L^2 when the longitudinal phase-mismatch Δk_L is 0. Because only the x -component of the pump wave was involved in the CDFG process, we rotated the half-wave plate to vary the power of the x -component of the pump wave to investigate the power dependence of the CDFG on the pump. Figure 4 shows the normalized power of CDFG depending on the power of the x -component of the pump wave, which fits to be a linear relationship.

Our scheme for realizing CDFG in normally dispersive materials is an alternative to the previous work in Ref. 14, in which backward reciprocal vectors provided by the quasi-phase-matching structure were used to accelerate the phase velocity of the nonlinear polarization wave. As for the quasi-phase-matched CDFG, domains with few-micron period are needed. For example, a domain period smaller than 3 μ m is needed to realize a 370-nm pumped CDFG in KTP, which is still a challenge in ferroelectric domain engineering. The method based on birefringence can reduce the requirements for fabricating short-period domain structures. Moreover, our work can be extended to waveguides, where mode dispersion engineering is more flexible, exploiting mode-matching to realize Cherenkov down-conversions.

To summarize, we put forward a scheme to realize a degenerate CDFG in the birefringent crystal KTP, where the pump (532 nm) and signal waves (1064 nm) were set to be along x and z polarizations, respectively, and CDFG was experimentally realized as expected. In addition to CDFG, CSHG and two types of Cherenkov THG were observed in the experiment as well. Some characteristics of the observed Cherenkov radiations, such as phase-matching diagrams, radiation angles, and CDFG intensity dependence on the pump wave, were investigated in detail.

The authors thank Professor Dragomir N. Neshev for beneficial discussions. This work was supported by the National Natural Science Foundation of China (Nos. 11274165, 91321312, 61222503, and 11404167), the Jiangsu

Science Foundation (No. BK20151374), and PAPD of Jiangsu Higher Education Institutions.

- ¹P. A. Cherenkov, Dokl. Akad. Nauk SSSR **2**, 451 (1934).
²P. K. Tien, R. Ulrich, and R. J. Martin, *Appl. Phys. Lett.* **17**, 447 (1970).
³K. Hayata, K. Yanagawa, and M. Koshiba, *Appl. Phys. Lett.* **56**, 206 (1990).
⁴H. Tamada, *IEEE J. Quantum Electron.* **27**, 502 (1991).
⁵N. An, H. J. Ren, Y. L. Zheng, X. W. Deng, and X. F. Chen, *Appl. Phys. Lett.* **100**, 221103 (2012).
⁶N. A. Sanford and J. M. Connors, *J. Appl. Phys.* **65**, 1429 (1989).
⁷K. Hayata and M. Koshiba, *J. Opt. Soc. Am. B* **8**, 449 (1991).
⁸C. D. Chen, J. Su, Y. Zhang, P. Xu, X. P. Hu, G. Zhao, Y. H. Liu, X. J. Lv, and S. N. Zhu, *Appl. Phys. Lett.* **97**, 161112 (2010).
⁹A. Fragemaan, V. Pasiskevicius, and F. Laurell, *Appl. Phys. Lett.* **85**, 375 (2004).
¹⁰Y. Zhang, Z. D. Gao, Z. Qi, S. N. Zhu, and N. B. Ming, *Phys. Rev. Lett.* **100**, 163904 (2008).
¹¹S. M. Saitiel, Y. Sheng, N. Voloch-Bloch, D. N. Neshev, W. Krolikowski, A. Arie, K. Koynov, and Y. S. Kivshar, *IEEE J. Quantum Electron.* **45**, 1465 (2009).
¹²X. W. Deng, H. J. Ren, Y. L. Zheng, K. Liu, and X. F. Chen, "Significantly enhanced second order nonlinearity in domain walls of ferroelectrics," preprint [arXiv:1005.2925v1](https://arxiv.org/abs/1005.2925v1) [physics.optics] (2010).
¹³Y. Sheng, A. Best, H. Butt, W. Krolikowski, A. Arie, and K. Koynov, *Opt. Express* **18**, 16539 (2010).
¹⁴C. D. Chen, X. P. Hu, Y. L. Xu, P. Xu, G. Zhao, and S. N. Zhu, *Appl. Phys. Lett.* **101**, 071113 (2012).
¹⁵H. J. Ren, X. W. Deng, Y. L. Zheng, N. An, and X. F. Chen, *Phys. Rev. Lett.* **108**, 223901 (2012).
¹⁶K. Kato, *IEEE J. Quantum Electron.* **28**, 1974 (1992).
¹⁷H. J. Ren, X. W. Deng, Y. L. Zheng, N. An, and X. F. Chen, *Opt. Lett.* **38**, 1993 (2013).
¹⁸M. Bass, C. M. DeCusatis, J. M. Enoch, V. Lakshminarayanan, G. F. Li, C. MacDonald, V. N. Mahajan, and E. V. Stryland, *Hand Book of Optics*, 3rd ed. (McGraw-Hill Professional, 2010), Vol. 4.